Int. J. Solids Structures Vol. 30, No. 1, pp. 1–17, 1993
Printed in Great Britain.

0020–7683/93 $5.00+ .00

BUCKLING OF RECTANGULAR MINDLIN PLATES WITH INTERNAL LINE SUPPORTS

C. M. WANG
Department of Civil Engineering, National University of Singapore, Kent Ridge 0511, Singapore

K. M. LIEW
School of Mechanical and Production Engineering, Nanyang Technological University, Nanyang Avenue 2263, Singapore

and

Y. XIANG and S. KITIPORNCHAI
Department of Civil Engineering, The University of Queensland, Queensland 4072, Australia

(*Received* 6 *August* 1991; *in revised form* 8 *June* 1992)

Abstract—This paper considers the elastic buckling of rectangular Mindlin plates under normal in-plane forces. The plates may have any number of internal line (straight or curved) supports that span between any two edges. Based on the energy functional derived from the incremental total potential energy approach, the newly developed pb-2 Rayleigh–Ritz method is applied for solution. The special feature of this method is the pb-2 Ritz function which consists of the product of (1) a two-dimensional polynomial function and (2) a basic function formed from taking the product of the equations of the boundaries and internal line supports; with each equation raised to appropriate powers as shown herein. The method is convenient for analysts since no discretization is required and very accurate results can be obtained. Buckling load intensity factors for rectangular plates with various boundary conditions and various thickness and aspect ratios are tabulated for designers. These may also serve as benchmark values for the testing of other numerical methods.

1. INTRODUCTION

Thick plates are important structural elements. They are used in a wide range of applications, including ship hulls, covers for cylinders, water tanks, doors of bunkers and hangars and armour plates for military vehicles and tanks. Thick plates may be analysed using classical thin plate theory, but because the effects of transverse shear deformation are neglected, deflections are underestimated while the natural frequencies and buckling loads are overestimated. These errors increase with increasing plate thickness. In thick plates, the shear strain distribution is somewhat complicated: thus there have been various higher-order shear deformation theories proposed [see, for example, Levinson (1980), Murthy (1981), Reddy (1984) and Senthilnathan *et al.* (1987)]. For computational simplicity, however, a constant transverse shear strain distribution through the plate thickness may be assumed. A shear correction factor, κ, is then introduced to compensate for the errors resulting from approximating the nonlinear shear strain distribution by the simple constant distribution. This first-order shear deformation plate theory was first proposed by Reissner (1945) and developed further by Mindlin (1951). Consequently, thick plates of this class have become known as Mindlin plates. It has been shown that such a first order shear deformation theory will suffice when determining natural frequencies and buckling loads (Lim *et al.*, 1989; Srinivas and Rao, 1970).

The objective of this paper is to determine the elastic buckling loads of rectangular Mindlin plates. This work is motivated by the fact that only a few buckling results for thick plates are found in the literature when compared to the extensive compilation of design charts and tables of buckling loads for rectangular thin plates with all kinds of boundary conditions [see, for example, Column Research Committee of Japan (1971), Libove (1962), Wang *et al.* (1992) and Liew and Wang (1992b)]. To generate the results, the newly developed pb-2 Rayleigh–Ritz method is employed (Liew and Wang, 1992a). Hitherto, the method has been applied only to thin plates and found to be a very convenient and accurate method. Its special feature lies in the definition of the Ritz function which takes the product

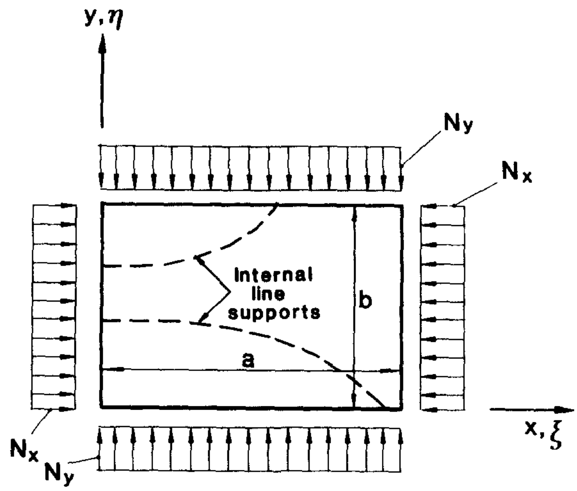

Fig. 1. Rectangular Mindlin plate with internal line (curved) supports under biaxial loading.

of a two-dimensional polynomial function (p-2) and the boundary expressions (b). Each of the equations of the boundary is raised to the power of 0, 1 or 2 corresponding to free, simply supported and clamped edges. Thus, pb-2 Ritz functions satisfy the geometric boundary conditions at the outset, making the Rayleigh–Ritz method applicable for plates of arbitrary shape and boundary conditions. The usual problem encountered in the Rayleigh–Ritz method of finding a suitable Ritz function is overcome because the function is automatically defined by the prescribed boundary shape and conditions. The simplicity of the method for the analysis of thick plates with internal supports is also presented in this paper.

2. ENERGY FUNCTIONAL FOR MINDLIN PLATES

Consider a flat, isotropic, thick, rectangular plate of uniform thickness, t; length, a; width, b; Young's modulus, E; shear modulus, G; and Poisson's ratio, ν. The plate may have any combination of prescribed supporting edges and may be supported internally by a given number of internal line (straight or curved) supports which span between any two edges. The plate is subject to normal in-plane loads N_x and N_y, as shown in Fig. 1. The problem is to determine the elastic buckling load of the plate.

Designating the present configuration of the Mindlin plate under the in-plane loads as C_1 and the next configuration of the plate as C_2, the incremental total potential energy functional is given by (Wang *et al.*, 1991)

$$F = \frac{1}{2}\int_V \Delta\varepsilon_L^T[B]\Delta\varepsilon_L \,dV + \int_V \tau^T \Delta\varepsilon_N \,dV - \frac{1}{2}\left[\int_S \Delta N_x u_0 \,dS + \int_S \Delta N_y v_0 \,dS\right], \qquad (1)$$

in which

V = volume of the plate at C_1;
$\Delta\varepsilon$ = incremental strain tensor from C_1 to C_2;
τ = stress tensor at C_1;
$[B]$ = material property matrix at C_1;
S = line along the four edges;
$u_0(x, y)$ = displacement along x in the middle surface from C_1 to C_2;
$v_0(x, y)$ = displacement along y in the middle surface from C_1 to C_2;
ΔN_x = increment in N_x from C_1 to C_2;
ΔN_y = increment in N_y from C_1 to C_2;

and the subscripts L and N denote linear and nonlinear components, respectively.

The displacement fields of the plate can be expressed as

$$u_i(x, y, z) = u_0(x, y) + z\theta_x(x, y), \tag{2a}$$

$$v_i(x, y, z) = v_0(x, y) + z\theta_y(x, y), \tag{2b}$$

$$w_i(x, y, z) = w_0(x, y), \tag{2c}$$

in which

$w_0(x, y)$ = displacement along z-axis in the middle surface from C_1 to C_2;
$\theta_x(x, y)$ = bending slope along y-axis from C_1 to C_2;
$\theta_y(x, y)$ = bending slope along x-axis from C_1 to C_2.

Note that θ_x and θ_y are independent variables and the transverse displacement, w_0, is assumed to be independent of z (i.e. no thickness deformation is allowed).

For buckling of the plate, $u_0(x, y)$ and $v_0(x, y)$ can be neglected (Wang *et al.*, 1991). Thus,

$$u_i(x, y, z) = z\theta_x(x, y), \tag{3a}$$

$$v_i(x, y, z) = z\theta_y(x, y), \tag{3b}$$

$$w_i(x, y, z) = w_0(x, y). \tag{3c}$$

In view of eqn (3) and the Green–Lagrange strain definition,

$$\Delta\varepsilon_L = \begin{Bmatrix} \varepsilon_{xxL} \\ \varepsilon_{yyL} \\ \gamma_{xyL} \\ \gamma_{xzL} \\ \gamma_{yzL} \end{Bmatrix} = \begin{Bmatrix} \dfrac{\partial u_i}{\partial x} \\ \dfrac{\partial v_i}{\partial y} \\ \dfrac{\partial u_i}{\partial y} + \dfrac{\partial v_i}{\partial x} \\ \dfrac{\partial u_i}{\partial z} + \dfrac{\partial w_i}{\partial x} \\ \dfrac{\partial v_i}{\partial z} + \dfrac{\partial w_i}{\partial y} \end{Bmatrix} = \begin{Bmatrix} z\dfrac{\partial \theta_x}{\partial x} \\ z\dfrac{\partial \theta_y}{\partial y} \\ z\left(\dfrac{\partial \theta_x}{\partial y} + \dfrac{\partial \theta_y}{\partial x}\right) \\ \theta_x + \dfrac{\partial w_0}{\partial x} \\ \theta_y + \dfrac{\partial w_0}{\partial y} \end{Bmatrix}, \tag{4}$$

$$\Delta\varepsilon_N = \begin{Bmatrix} \varepsilon_{xxN} \\ \varepsilon_{yyN} \\ \gamma_{xyN} \\ \gamma_{xzN} \\ \gamma_{yzN} \end{Bmatrix} = \begin{Bmatrix} \dfrac{1}{2}\left(\dfrac{\partial w_i}{\partial x}\right)^2 \\ \dfrac{1}{2}\left(\dfrac{\partial w_i}{\partial y}\right)^2 \\ \dfrac{\partial w_i}{\partial x}\dfrac{\partial w_i}{\partial y} \\ \dfrac{\partial w_i}{\partial x}\dfrac{\partial w_i}{\partial z} \\ \dfrac{\partial w_i}{\partial y}\dfrac{\partial w_i}{\partial z} \end{Bmatrix} = \begin{Bmatrix} \dfrac{1}{2}\left(\dfrac{\partial w_0}{\partial x}\right)^2 \\ \dfrac{1}{2}\left(\dfrac{\partial w_0}{\partial y}\right)^2 \\ \dfrac{\partial w_0}{\partial x}\dfrac{\partial w_0}{\partial y} \\ 0 \\ 0 \end{Bmatrix}. \tag{5}$$

Note that higher order terms involving the in-plane displacements in $\Delta\varepsilon_N$ are neglected.

Moreover, the material property matrix is given by

$$[B] = \begin{bmatrix} \frac{E}{1-\nu^2} & \frac{\nu E}{1-\nu^2} & 0 & 0 & 0 \\ \frac{\nu E}{1-\nu^2} & \frac{E}{1-\nu^2} & 0 & 0 & 0 \\ 0 & 0 & G & 0 & 0 \\ 0 & 0 & 0 & \kappa G & 0 \\ 0 & 0 & 0 & 0 & \kappa G \end{bmatrix}, \tag{6}$$

in which $G = E/[2(1+\nu)]$ and κ is the shear correction factor. In view of the parabolic variation of the transverse shear stresses through the plate thickness, an approximate correction factor, $\kappa = 5/6$ (Reissner, 1945), is introduced to compensate for the errors when assuming a constant shear strain distribution.

The stress tensor, τ, is given by

$$\tau^T = [\sigma_{xx} \quad \sigma_{yy} \quad \sigma_{xy} \quad \sigma_{xz} \quad \sigma_{yz}]. \tag{7}$$

Substituting eqns (2)–(7) into eqn (1) yields

$$F = \frac{1}{2}\int_V \left\{ \frac{Ez^2}{1-\nu^2}\left[\left(\frac{\partial \theta_x}{\partial x} + \frac{\partial \theta_y}{\partial y}\right)^2 - 2(1-\nu)\left(\frac{\partial \theta_x}{\partial x}\frac{\partial \theta_y}{\partial y} - \frac{1}{4}\left(\frac{\partial \theta_x}{\partial y} + \frac{\partial \theta_y}{\partial x}\right)^2\right)\right] \right.$$
$$\left. + \kappa G\left[\left(\theta_x + \frac{\partial w_0}{\partial x}\right)^2 + \left(\theta_y + \frac{\partial w_0}{\partial y}\right)^2\right] - \left[\sigma_{xx}\left(\frac{\partial w_0}{\partial x}\right)^2 + \sigma_{yy}\left(\frac{\partial w_0}{\partial y}\right)^2 + 2\sigma_{xy}\frac{\partial w_0}{\partial x}\frac{\partial w_0}{\partial y}\right]\right\} \mathrm{d}V. \tag{8}$$

Note that if $\theta_x = -\partial w_0/\partial x$ and $\theta_y = -\partial w_0/\partial y$, eqn (8) reduces to the well-known energy functional for thin plates.

For generality and convenience, the coordinates are normalized with respect to the plate dimensions, i.e.

$$\xi = \frac{x}{a}, \quad \eta = \frac{y}{b}. \tag{9}$$

By taking C_1 as the configuration at the state of incipient buckling and C_2 as the configuration just after buckling, $\sigma_{xx} = -N_x/t$, $\sigma_{yy} = -N_y/t$ and $\sigma_{xy} = 0$. The integration of eqn (8) with respect to z yields the following energy functional expression

$$F = \frac{1}{2}\int_0^1\int_0^1 \left\{ D\left[\left(\frac{1}{a}\frac{\partial \theta_x}{\partial \xi} + \frac{1}{b}\frac{\partial \theta_y}{\partial \eta}\right)^2 - 2(1-\nu)\left(\frac{1}{ab}\frac{\partial \theta_x}{\partial \xi}\frac{\partial \theta_y}{\partial \eta} - \frac{1}{4}\left(\frac{1}{b}\frac{\partial \theta_x}{\partial \eta} + \frac{1}{a}\frac{\partial \theta_y}{\partial \xi}\right)^2\right)\right] \right.$$
$$\left. + \kappa Gt\left[\left(\theta_x + \frac{1}{a}\frac{\partial w_0}{\partial \xi}\right)^2 + \left(\theta_y + \frac{1}{b}\frac{\partial w_0}{\partial \eta}\right)^2\right] - \left[N_x\left(\frac{1}{a}\frac{\partial w_0}{\partial \xi}\right)^2 + N_y\left(\frac{1}{b}\frac{\partial w_0}{\partial \eta}\right)^2\right]\right\} ab\,\mathrm{d}\xi\,\mathrm{d}\eta, \tag{10}$$

in which $D = Et^3/[12(1-\nu^2)]$.

3. BOUNDARY CONDITIONS FOR MINDLIN PLATES

The following support conditions for Mindlin plates are considered (Huang, 1989):

(1) *Free edge* (F)

For this type of edge condition,

$$Q_n = 0, \quad M_n = 0 \quad \text{and} \quad M_{nt} = 0, \tag{11}$$

in which Q_n is the shearing force, M_n is the bending moment and M_{nt} is the twisting moment.

(2) *Simply-supported edge* (S *and* S*)

There are two kinds of simply-supported edges in the Mindlin plate theory. The first kind (S) requires

$$w_0 = 0, \quad M_n = 0 \quad \text{and} \quad \theta_t = 0 \tag{12}$$

in which θ_t is the rotation of the mid-plane normal in the tangent plane tz to the plate boundary.

The boundary conditions for the second kind (S*) are such that

$$w_0 = 0, \quad M_n = 0 \quad \text{and} \quad M_{nt} = 0. \tag{13}$$

(3) *Internal curved supports*

For an internal curve support along its length, the following conditions are to be met:

$$\begin{aligned} &w_0 = 0, \quad \frac{\partial w_0^-}{\partial n} = \frac{\partial w_0^+}{\partial n}, \quad \theta_n^- = \theta_n^+, \\ &\theta_t^- = \theta_t^+, \quad M_n^- = M_n^+, \quad M_{nt}^- = M_{nt}^+, \end{aligned} \tag{14}$$

in which the superscripts $-$ and $+$ indicate positions to the left and right of the support.

4. pb-2 RAYLEIGH–RITZ METHOD

For Mindlin plates, the transverse deflection and bending slopes may be parameterized by

$$w_0(\xi, \eta) = \sum_{i=1}^{m} c_i \phi_i(\xi, \eta), \tag{15a}$$

$$\theta_x(\xi, \eta) = \sum_{i=1}^{n} d_i \psi_{xi}(\xi, \eta), \tag{15b}$$

$$\theta_y(\xi, \eta) = \sum_{i=1}^{l} e_i \psi_{yi}(\xi, \eta), \tag{15c}$$

where

$$\phi_i(\xi, \eta) = f_i(\xi, \eta)\phi_1(\xi, \eta), \tag{16a}$$

$$\psi_{xi}(\xi, \eta) = f_i(\xi, \eta)\psi_{x1}(\xi, \eta), \tag{16b}$$

$$\psi_{yi}(\xi, \eta) = f_i(\xi, \eta)\psi_{y1}(\xi, \eta). \tag{16c}$$

f_i is a two-dimensional polynomial function generated as follows:

$$f_i(\xi, \eta) = \xi^r \eta^s (\cos^2 \pi q) + \xi^s \eta^r (\sin^2 \pi q), \tag{17a}$$

where

$$r = \lceil \sqrt{i-1} \rceil, \tag{17b}$$

$$q = \frac{i - r^2 - 1}{2}, \tag{17c}$$

$$s = q(\cos^2 \pi q) + (q - \tfrac{1}{2})(\sin^2 \pi q). \tag{17d}$$

$\lceil\ \rceil$ is a function which denotes the greatest integer less than the argument, for example $\lceil\sqrt{2}\rceil = 1$. ϕ_1, ψ_{x1} and ψ_{y1} are basic functions which only need to satisfy the kinematic boundary conditions [eqns (11)–(14)]. The basic function for the deflection can be expressed as (Liew and Wang, 1992b):

$$\phi_1 = \left\{\prod_{i=1}^{4} [\Gamma_i(\xi, \eta)]^{\Omega_i}\right\} \left\{\prod_{j=1}^{n_i} [\Lambda_j(\xi, \eta)]^{\Phi_j}\right\}, \tag{18}$$

where n_i is the number of internal line (straight or curved) supports, Γ_i the boundary equation of the ith supporting edge, Λ_j the equation of the jth internal support. Ω_i is dependent on the support edge condition, such that

$$\Omega_i = 0 \quad \text{if the } i\text{th edge is free (F)}, \tag{19a}$$

$$\Omega_i = 1 \quad \text{if the } i\text{th edge is simply supported (S and S*)}, \tag{19b}$$

while

$$\Phi_j = 0 \quad \text{if the } j\text{th internal support is removed}, \tag{19c}$$

$$\Phi_j = 1 \quad \text{if the } j\text{th internal support is present}. \tag{19d}$$

The basic functions for the bending slopes can be expressed as

$$\psi_{x1} = \prod_{i=1}^{4} [\Gamma_i(\xi, \eta)]^{\Omega_i}, \tag{20a}$$

$\Omega_i = 0$ if the ith edge is free (F) or simply supported (S*) or simply supported (S) in the y-direction, (20b)

$\Omega_i = 1$ if the ith edge is simply supported (S) in the x-direction; (20c)

$$\psi_{y1} = \prod_{i=1}^{4} [\Gamma_i(\xi, \eta)]^{\Omega_i}, \tag{21a}$$

$\Omega_i = 0$ if the ith edge is free (F) or simply supported (S*) or simply supported (S) in the x-direction, (21b)

$\Omega_i = 1$ if the ith edge is simply supported (S) in the y-direction. (21c)

Applying the Rayleigh–Ritz method leads to

$$[K]\begin{Bmatrix} \{c\} \\ \{d\} \\ \{e\} \end{Bmatrix} = \{0\}, \tag{22}$$

in which

$$\{c\} = \begin{Bmatrix} c_1 \\ c_2 \\ \vdots \\ c_m \end{Bmatrix}, \quad \{d\} = \begin{Bmatrix} d_1 \\ d_2 \\ \vdots \\ d_n \end{Bmatrix}, \quad \{e\} = \begin{Bmatrix} e_1 \\ e_2 \\ \vdots \\ e_l \end{Bmatrix}, \tag{23}$$

$$[K] = \begin{bmatrix} [K_{cc}] & [K_{cd}] & [K_{ce}] \\ & [K_{dd}] & [K_{de}] \\ \text{symmetric} & & [K_{ee}] \end{bmatrix}, \tag{24}$$

$$K_{ccij} = \frac{b}{a}(\kappa Gt - N_x)\int_0^1\int_0^1 \frac{\partial\phi_i}{\partial\xi}\frac{\partial\phi_j}{\partial\xi}\,\mathrm{d}\xi\,\mathrm{d}\eta + \frac{a}{b}(\kappa Gt - N_y)\int_0^1\int_0^1 \frac{\partial\phi_i}{\partial\eta}\frac{\partial\phi_j}{\partial\eta}\,\mathrm{d}\xi\,\mathrm{d}\eta,$$
$$i = 1,2,\ldots,m;\ j = 1,2,\ldots,m, \quad (25)$$

$$K_{cdij} = b\kappa Gt\int_0^1\int_0^1 \frac{\partial\phi_i}{\partial\xi}\psi_{xj}\,\mathrm{d}\xi\,\mathrm{d}\eta, \quad i = 1,2,\ldots,m;\ j = 1,2,\ldots,n, \quad (26)$$

$$K_{ceij} = a\kappa Gt\int_0^1\int_0^1 \frac{\partial\phi_i}{\partial\eta}\psi_{yj}\,\mathrm{d}\xi\,\mathrm{d}\eta, \quad i = 1,2,\ldots,m;\ j = 1,2,\ldots,l, \quad (27)$$

$$K_{ddij} = \frac{b}{a}D\int_0^1\int_0^1 \frac{\partial\psi_{xi}}{\partial\xi}\frac{\partial\psi_{xj}}{\partial\xi}\,\mathrm{d}\xi\,\mathrm{d}\eta + \frac{a}{b}D\frac{(1-\nu)}{2}\int_0^1\int_0^1 \frac{\partial\psi_{xi}}{\partial\eta}\frac{\partial\psi_{xj}}{\partial\eta}\,\mathrm{d}\xi\,\mathrm{d}\eta$$
$$+ab\kappa Gt\int_0^1\int_0^1 \psi_{xi}\psi_{xj}\,\mathrm{d}\xi\,\mathrm{d}\eta, \quad i = 1,2,\ldots,n;\ j = 1,2,\ldots,n, \quad (28)$$

$$K_{deij} = \nu D\int_0^1\int_0^1 \frac{\partial\psi_{xi}}{\partial\xi}\frac{\psi_{yj}}{\partial\eta}\,\mathrm{d}\xi\,\mathrm{d}\eta + D\frac{(1-\nu)}{2}\int_0^1\int_0^1 \frac{\partial\psi_{xi}}{\partial\eta}\frac{\partial\psi_{yj}}{\partial\xi}\,\mathrm{d}\xi\,\mathrm{d}\eta,$$
$$i = 1,2,\ldots,n;\ j = 1,2,\ldots,l, \quad (29)$$

$$K_{eeij} = \frac{a}{b}D\int_0^1\int_0^1 \frac{\partial\psi_{yi}}{\partial\eta}\frac{\partial\psi_{yj}}{\partial\eta}\,\mathrm{d}\xi\,\mathrm{d}\eta + \frac{b}{a}D\frac{(1-\nu)}{2}\int_0^1\int_0^1 \frac{\partial\psi_{yi}}{\partial\xi}\frac{\partial\psi_{yj}}{\partial\xi}\,\mathrm{d}\xi\,\mathrm{d}\eta$$
$$+ab\kappa Gt\int_0^1\int_0^1 \psi_{yi}\psi_{yj}\,\mathrm{d}\xi\,\mathrm{d}\eta, \quad i = 1,2,\ldots,l;\ j = 1,2,\ldots,l. \quad (30)$$

The buckling load intensity factor, $k = \sigma tb^2/(\pi^2 D)$, is obtained by solving the generalized eigenvalue problem defined by eqn (22). Note that by making use of the special features of polynomial functions, a Fortran program has been written to perform the differentiation and integration of polynomial functions symbolically so long as the limits of the integration are constant. After the stiffness matrix $[K]$ is obtained, the first eigenvalues of N_x and N_y in eqn (22) are determined using the SKYFAC subroutine (Felippa, 1975) by the iteration method.

5. NUMERICAL RESULTS

Rectangular plates of Poisson's ratio $\nu = 0.3$, various aspect ratios (a/b), thickness to width ratios (t/b) and different combinations of supporting conditions are considered. The plates are subjected to either uniaxial compression ($\sigma_x = \sigma$, $\sigma_y = 0$) or biaxial compression ($\sigma_x = \sigma_y = \sigma$). Figure 2 summarizes the 32 loading and boundary conditions considered.

Convergence studies are carried out on Cases 3, 7, 9, 13, 28 and 32 (see Fig. 2) to establish the number of polynomial terms required for accurate solution. The results are presented in Tables 1–2. It can be seen that for Cases 3, 7, 9 and 13, $m = n = l = 60$ is sufficient to provide accurate results while $m = n = l = 100$ is required for Cases 28 and 32. Moreover, fewer terms are needed for aspect ratios $a/b = 0.5$ and 1.0 but more terms should be taken for aspect ratio $a/b = 2.5$. The buckling load intensity factors converge more rapidly for plates subject to biaxial compression than the ones subject to uniaxial compression. In the present study, $m = n = l = 100$ has been adopted to generate all results.

Figures 3–5 present the relations between buckling load intensity factor k and aspect ratio a/b with different thickness to width ratio t/b for Cases 3, 7, 19, 23, 27 and 31. It can be seen that the effect of shear deformation on buckling load is more pronounced for plates with large thickness to width ratio t/b and small aspect ratio a/b. The buckling factors

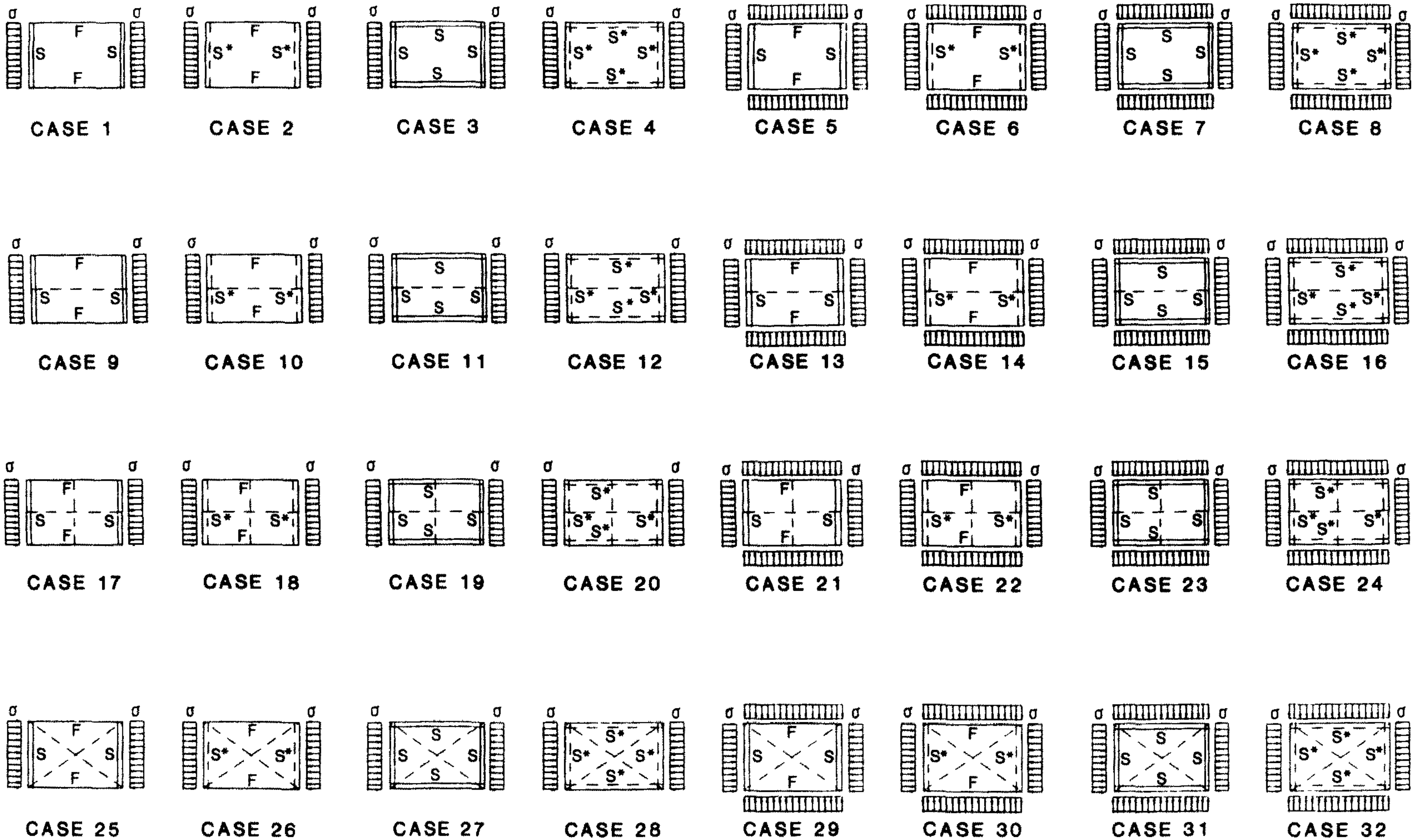

Fig. 2. Loading and boundary conditions of Mindlin plates analysed.

Table 1. Convergence study of buckling load intensity factor, $k = \sigma t b^2/(\pi^2 D)$, of Mindlin plates for Cases 3, 7 and 9

		Case 3			Case 7			Case 9		
		t/b			t/b			t/b		
a/b	$m = n = l$	0.0010	0.1000	0.2000	0.0010	0.1000	0.2000	0.0010	0.1000	0.2000
0.5	40	6.2500	5.4777	3.9962	4.9999	4.3822	3.1970	5.6087	4.8852	3.6071
	60	6.2500	5.4777	3.9962	4.9999	4.3822	3.1970	5.6063	4.8681	3.6028
	80	6.2500	5.4777	3.9962	4.9999	4.3822	3.1970	5.6063	4.8675	3.6025
	90	6.2500	5.4777	3.9962	4.9999	4.3822	3.1970	5.6063	4.8634	3.6022
	95	6.2500	5.4777	3.9962	4.9999	4.3822	3.1970	5.6063	4.8634	3.6022
	100	6.2500	5.4777	3.9962	4.9999	4.3822	3.1970	5.6063	4.8634	3.6022
1.0	40	4.0000	3.7865	3.2637	2.0000	1.8932	1.6319	2.6726	2.4894	2.1615
	60	4.0000	3.7865	3.2637	2.0000	1.8932	1.6319	2.6726	2.4760	2.1584
	80	4.0000	3.7865	3.2637	2.0000	1.8932	1.6319	2.6725	2.4758	2.1583
	90	4.0000	3.7865	3.2637	2.0000	1.8932	1.6319	2.6725	2.4732	2.1581
	95	4.0000	3.7865	3.2637	2.0000	1.8932	1.6319	2.6725	2.4732	2.1581
	100	4.0000	3.7865	3.2637	2.0000	1.8932	1.6319	2.6725	2.4732	2.1581
2.5	40	4.1682	3.8964	3.2589	1.1600	1.1233	1.0258	1.8569	1.7529	1.6058
	60	4.1351	3.8690	3.2427	1.1600	1.1233	1.0258	1.8569	1.7406	1.6032
	80	4.1351	3.8690	3.2427	1.1600	1.1233	1.0258	1.8569	1.7406	1.6032
	90	4.1345	3.8683	3.2423	1.1600	1.1233	1.0258	1.8569	1.7383	1.6030
	95	4.1344	3.8683	3.2422	1.1600	1.1233	1.0258	1.8569	1.7383	1.6030
	100	4.1344	3.8683	3.2422	1.1600	1.1233	1.0258	1.8569	1.7383	1.6030

decrease with increasing aspect ratios in Cases 7, 23, 27 and 31. This trend occurs more significantly for plates with small thickness to width ratio t/b and less significantly for plates with large thickness to width ratio. It is evident that in Cases 3 and 19, the buckling shapes of the plates shift from lower modes to higher ones as the aspect ratio a/b increases. The locations of the kinks occur earlier when the plates are thicker.

Tables 3–6 present the buckling load intensity factors for plates with four different boundary conditions, i.e. FSFS, FS*FS*, SSSS, S*S*S*S* under uniaxial and biaxial loadings. For Case 3, the buckling results for the square plate ($a/b = 1$) are in total agreement with available closed form solutions (Hinton, 1988) of 4.000, 3.944, 3.786, 3.264 for $t/b = 0.001, 0.05, 0.10, 0.20$, respectively. These values are found to be only a few percent different from (1) Roufaeil and Dawe (1982) solutions which incorporate higher order terms in the nonlinear strain components, $\Delta\varepsilon_N$ and (2) the exact three-dimensional solutions given by Srinivas and Rao (1969). The close agreement in results confirms the sufficiency

Table 2. Convergence study of buckling load intensity factor, $k = \sigma t b^2/(\pi^2 D)$, of Mindlin plates for Cases 13, 28 and 32

		Case 13			Case 28			Case 32		
		t/b			t/b			t/b		
a/b	$m = n = l$	0.0010	0.1000	0.2000	0.0010	0.1000	0.2000	0.0010	0.1000	0.2000
0.5	40	4.2207	3.6126	2.6316	39.448	19.610	7.8599	30.993	15.202	6.3415
	60	4.2205	3.5790	2.6219	39.212	19.381	7.8127	29.807	14.525	6.2110
	80	4.2205	3.5775	2.6211	38.455	19.370	7.7766	28.480	14.345	6.1775
	90	4.2204	3.5704	2.6206	38.453	19.359	7.7747	28.476	14.313	6.1703
	95	4.2204	3.5703	2.6206	38.453	19.358	7.7731	28.473	14.307	6.1689
	100	4.2204	3.5703	2.6206	38.451	19.356	7.7698	28.473	14.302	6.1678
1.0	40	1.1899	1.0958	0.9431	19.955	13.948	7.0830	10.238	7.7687	4.6179
	60	1.1899	1.0871	0.9410	19.885	13.071	6.7402	10.222	7.6228	4.5721
	80	1.1899	1.0871	0.9410	18.410	12.950	6.7093	10.004	7.6138	4.5710
	90	1.1898	1.0854	0.9409	18.398	12.835	6.6866	10.004	7.6118	4.5703
	95	1.1898	1.0854	0.9409	18.398	12.831	6.6857	10.004	7.6113	4.5703
	100	1.1898	1.0854	0.9409	18.396	12.824	6.6844	10.003	7.6112	4.5701
2.5	40	0.2150	0.2024	0.1849	19.447	11.882	6.3378	7.6704	5.8094	3.6053
	60	0.2150	0.2008	0.1846	16.268	10.531	5.8752	7.0295	5.3829	3.4088
	80	0.2150	0.2008	0.1846	14.222	9.5184	5.5325	6.5644	5.1887	3.3278
	90	0.2150	0.2005	0.1846	12.352	9.1173	5.4315	6.5637	5.1806	3.3247
	95	0.2150	0.2005	0.1846	12.319	9.0842	5.4237	6.5637	5.1782	3.3235
	100	0.2150	0.2005	0.1846	12.318	9.0782	5.4225	6.5635	5.1748	3.3225

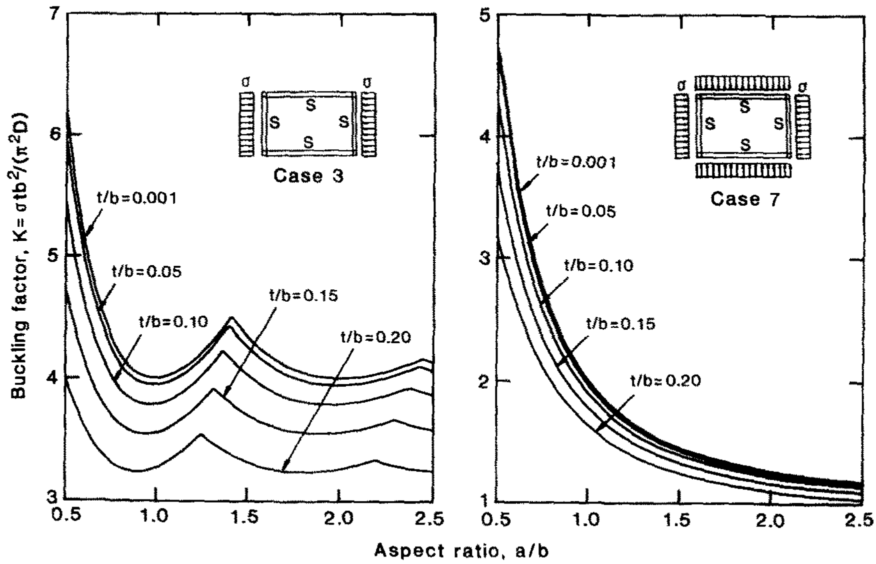

Fig. 3. Buckling factor k versus aspect ratio a/b of Mindlin plates with various thickness to width ratio t/b for Cases 3 and 7.

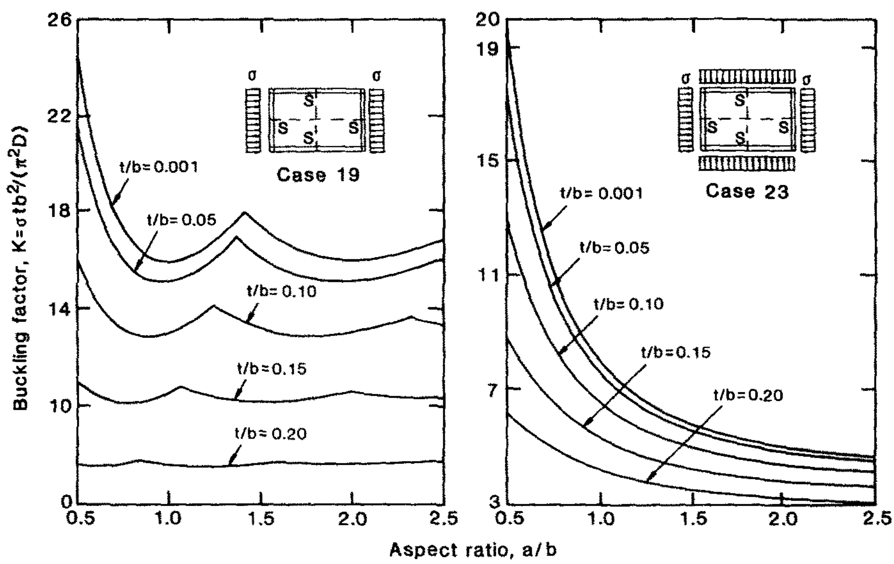

Fig. 4. Buckling factor k versus aspect ratio a/b of Mindlin plates with various thickness to width ratio t/b for Cases 19 and 23.

of the Mindlin theory in providing reasonably accurate solutions without having to consider more complicated higher-order theories or three-dimensional analysis.

Sample results for Case 7 ($t/b = 0.1$) are in total agreement with Hinton's closed form solutions (Hinton, 1988) of 1.893, 1.568, 1.388, 1.279 and 1.207 for aspect ratios, $a/b = 1.00$, 1.25, 1.50, 1.75 and 2.00, respectively. As expected, the buckling load intensity factor decreases with increasing thickness to width ratio, t/b due to the effect of shear deformation. And this effect is more pronounced for small aspect ratios than for large ratios. The buckling load intensity factor decreases with increasing aspect ratio a/b except for Cases 3 and 4, which contain the shifting of the buckling modes from lower ones to higher ones. Note that the shifting between modes is the peak shown in Fig. 3.

Tables 7–10 present the buckling load intensity factors for plates with a centrally located longitudinal line support [where $\Lambda_1 = \eta - 0.5$ for eqn (18)]. The buckling load intensity factors decrease with increasing t/b values, the same as the cases in Tables 3–6.

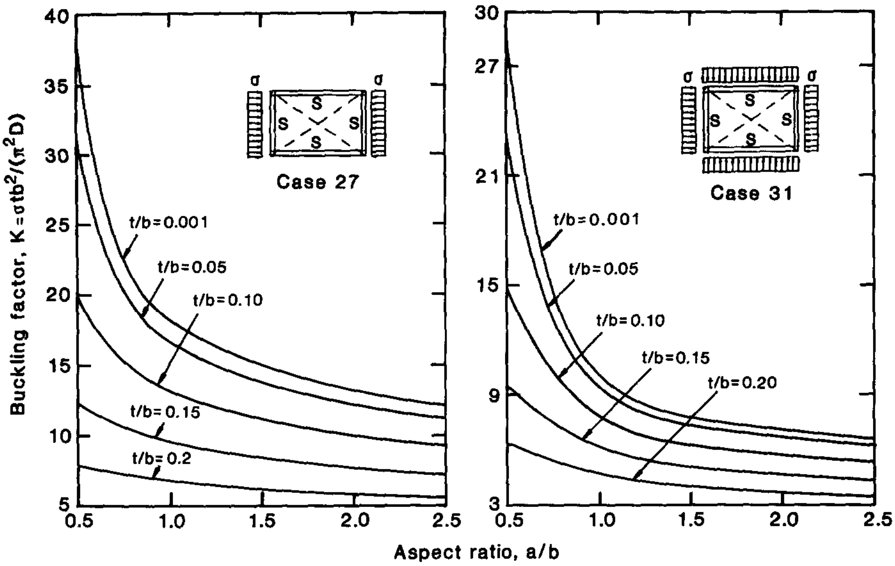

Fig. 5. Buckling factor k versus aspect ratio a/b of Mindlin plates with various thickness to width ratio t/b for Cases 27 and 31.

Table 3. Buckling load intensity factor, $k = \sigma t b^2/(\pi^2 D)$, of Mindlin plates having SFSF boundary conditions subject to uni- and bi-axial loadings

t/b			Case 1					Case 5		
a/b	0.0010	0.0500	0.1000	0.1500	0.2000	0.0010	0.0500	0.1000	0.1500	0.2000
0.5000	3.8926	3.7773	3.4854	3.0956	2.6797	3.8099	3.6738	3.3607	2.9635	2.5516
0.6250	2.4766	2.4271	2.3005	2.1218	1.9161	2.4219	2.3619	2.2242	2.0403	1.8344
0.7500	1.7103	1.6852	1.6217	1.5295	1.4186	1.6722	1.6413	1.5716	1.4761	1.3643
0.8750	1.2499	1.2357	1.2003	1.1484	1.0840	1.2225	1.2049	1.1659	1.1118	1.0467
1.0000	0.9523	0.9436	0.9223	0.8908	0.8512	0.9322	0.9214	0.8979	0.8651	0.8249
1.1250	0.7491	0.7434	0.7298	0.7097	0.6841	0.7341	0.7271	0.7120	0.6911	0.6650
1.2500	0.6043	0.6004	0.5913	0.5779	0.5606	0.5929	0.5882	0.5781	0.5641	0.5466
1.3750	0.4977	0.4949	0.4885	0.4792	0.4672	0.4889	0.4856	0.4786	0.4689	0.4566
1.5000	0.4168	0.4148	0.4103	0.4036	0.3949	0.4100	0.4076	0.4026	0.3957	0.3869
1.6250	0.3542	0.3527	0.3493	0.3444	0.3380	0.3488	0.3470	0.3434	0.3383	0.3318
1.7500	0.3046	0.3035	0.3009	0.2972	0.2925	0.3003	0.2990	0.2963	0.2924	0.2876
1.8750	0.2648	0.2639	0.2619	0.2591	0.2554	0.2613	0.2603	0.2582	0.2553	0.2516
2.0000	0.2322	0.2315	0.2300	0.2278	0.2250	0.2295	0.2286	0.2270	0.2248	0.2219
2.1250	0.2054	0.2048	0.2036	0.2019	0.1996	0.2031	0.2024	0.2012	0.1994	0.1971
2.2500	0.1829	0.1824	0.1815	0.1801	0.1783	0.1810	0.1805	0.1795	0.1781	0.1762
2.3750	0.1639	0.1635	0.1628	0.1616	0.1602	0.1624	0.1619	0.1611	0.1600	0.1585
2.5000	0.1477	0.1474	0.1468	0.1459	0.1447	0.1464	0.1461	0.1454	0.1445	0.1433

The effect of shear deformation on buckling load is more pronounced for the plates with a centrally located longitudinal line support than the ones without internal line support.

Tables 11–14 present the buckling load intensity factors for plates with two centrally located transverse and longitudinal supports [where $\Lambda_1 = \eta - 0.5$ and $\Lambda_2 = \xi - 0.5$ for eqn (18)]. For such internally supported plates, the decrease in the buckling intensity factors with respect to t/b ratios is more significant, especially when the aspect ratio is small.

Tables 15–18 present the buckling load intensity factors for plates with two diagonal internal line supports (where $\Lambda_1 = \eta - \xi$ and $\Lambda_2 = \eta + \xi - 1$). The buckling load intensity factors for this kind of internally supported plate are relatively sensitive to the variation of t/b and a/b ratios. For example, the buckling load intensity factors can decrease by as much as four- to five-fold when varying t/b from 0.001 to 0.2 for $a/b = 0.5$.

Note that the buckling load intensity factors for plates with S supports and the corresponding ones with S* supports are about the same value when the plate thickness is small (i.e. $t/b = 0.001$) but the factors deviate from each other with increasing t/b ratios.

Table 4. Buckling load intensity factor, $k = \sigma t h^2/(\pi^2 D)$, of Mindlin plates having S*FS*F boundary conditions subject to uni- and bi-axial loadings

t/b			Case 2					Case 6		
a/b	0.0010	0.0500	0.1000	0.1500	0.2000	0.0010	0.0500	0.1000	0.1500	0.2000
0.5000	3.8926	3.7693	3.4710	3.0778	2.6613	3.8098	3.6280	3.2388	2.6985	2.2230
0.6250	2.4766	2.4226	2.2920	2.1109	1.9043	2.4219	2.3424	2.1762	1.9182	1.6346
0.7500	1.7102	1.6825	1.6164	1.5226	1.4109	1.6722	1.6317	1.5491	1.4331	1.2469
0.8750	1.2499	1.2340	1.1968	1.1438	1.0789	1.2225	1.1999	1.1542	1.0942	0.9828
1.0000	0.9523	0.9425	0.9199	0.8877	0.8477	0.9322	0.9185	0.8912	0.8553	0.7955
1.1250	0.7491	0.7427	0.7282	0.7075	0.6816	0.7341	0.7254	0.7081	0.6853	0.6578
1.2500	0.6043	0.5999	0.5902	0.5763	0.5589	0.5929	0.5872	0.5757	0.5606	0.5423
1.3750	0.4977	0.4945	0.4877	0.4781	0.4659	0.4889	0.4849	0.4770	0.4666	0.4539
1.5000	0.4168	0.4146	0.4097	0.4028	0.3940	0.4100	0.4072	0.4016	0.3942	0.3851
1.6250	0.3542	0.3525	0.3489	0.3438	0.3374	0.3488	0.3467	0.3426	0.3372	0.3306
1.7500	0.3046	0.3033	0.3006	0.2968	0.2920	0.3003	0.2988	0.2958	0.2917	0.2867
1.8750	0.2648	0.2638	0.2617	0.2588	0.2550	0.2613	0.2601	0.2578	0.2548	0.2510
2.0000	0.2322	0.2315	0.2298	0.2276	0.2247	0.2295	0.2285	0.2268	0.2244	0.2214
2.1250	0.2054	0.2047	0.2034	0.2017	0.1994	0.2031	0.2024	0.2010	0.1991	0.1968
2.2500	0.1829	0.1824	0.1814	0.1799	0.1781	0.1810	0.1804	0.1793	0.1778	0.1760
2.3750	0.1639	0.1635	0.1627	0.1615	0.1600	0.1624	0.1619	0.1610	0.1598	0.1583
2.5000	0.1477	0.1474	0.1467	0.1458	0.1446	0.1464	0.1461	0.1453	0.1444	0.1431

Table 5. Buckling load intensity factor, $k = \sigma t b^2/(\pi^2 D)$, of Mindlin plates having SSSS boundary conditions subject to uni- and bi-axial loadings

t/b			Case 3					Case 7		
a/b	0.0010	0.0500	0.1000	0.1500	0.2000	0.0010	0.0500	0.1000	0.1500	0.2000
0.5000	6.2500	6.0372	5.4777	4.7448	3.9962	4.9999	4.8298	4.3822	3.7958	3.1970
0.6250	4.9506	4.8294	4.4990	4.0385	3.5323	3.5600	3.4728	3.2352	2.9041	2.5401
0.7500	4.3403	4.2569	4.0250	3.6900	3.3048	2.7778	2.7244	2.5760	2.3616	2.1151
0.8750	4.0718	4.0066	3.8231	3.5520	3.2313	2.3061	2.2692	2.1653	2.0118	1.8301
1.0000	4.0000	3.9444	3.7865	3.5496	3.2637	2.0000	1.9722	1.8932	1.7748	1.6319
1.1250	4.0558	4.0052	3.8609	3.6421	3.3744	1.7901	1.7678	1.7041	1.6075	1.4894
1.2500	4.2025	4.1545	4.0168	3.8065	3.5323	1.6400	1.6213	1.5675	1.4854	1.3840
1.3750	4.4195	4.3724	4.2178	3.8310	3.3952	1.5289	1.5126	1.4657	1.3937	1.3040
1.5000	4.3403	4.2569	4.0250	3.6900	3.3048	1.4444	1.4299	1.3879	1.3232	1.2421
1.6250	4.1749	4.1022	3.8985	3.6005	3.2524	1.3787	1.3654	1.3271	1.2678	1.1932
1.7500	4.0718	4.0066	3.8231	3.5520	3.2313	1.3265	1.3142	1.2787	1.2236	1.1539
1.8750	4.0167	3.9571	3.7883	3.5370	3.2363	1.2844	1.2729	1.2396	1.1877	1.1219
2.0000	4.0000	3.9444	3.7865	3.5496	3.2637	1.2500	1.2391	1.2074	1.1582	1.0955
2.1250	4.0147	3.9620	3.8120	3.5827	3.3105	1.2215	1.2110	1.1808	1.1336	1.0735
2.2500	4.0558	4.0052	3.8609	3.6421	3.3048	1.1975	1.1875	1.1584	1.1130	1.0550
2.3750	4.1193	4.0703	3.9299	3.6253	3.2661	1.1773	1.1676	1.1395	1.0955	1.0393
2.5000	4.1344	4.0645	3.8683	3.5802	3.2422	1.1600	1.1506	1.1233	1.0805	1.0258

Table 6. Buckling load intensity factor, $k = \sigma t b^2/(\pi^2 D)$, of Mindlin plates having S*S*S*S* boundary conditions subject to uni- and bi-axial loadings

t/b			Case 4					Case 8		
a/b	0.0010	0.0500	0.1000	0.1500	0.2000	0.0010	0.0500	0.1000	0.1500	0.2000
0.5000	6.2496	5.8121	5.1186	4.3680	3.6626	4.9997	4.6493	4.0938	3.4932	2.9291
0.6250	4.9503	4.6324	4.1605	3.6558	3.1674	3.5598	3.3309	2.9912	2.6281	2.2769
0.7500	4.3400	4.0807	3.7055	3.3112	2.9253	2.7776	2.6115	2.3712	2.1188	1.8718
0.8750	4.0716	3.8464	3.5200	3.1806	2.8458	2.3060	2.1785	1.9935	1.8013	1.6118
1.0000	3.9998	3.7968	3.4971	3.1861	2.8767	1.9999	1.8984	1.7487	1.5933	1.4388
1.1250	4.0556	3.8676	3.5831	3.2863	2.9877	1.7901	1.7072	1.5818	1.4511	1.3197
1.2500	4.2024	4.0250	3.7488	3.4572	3.1604	1.6399	1.5709	1.4634	1.3502	1.2351
1.3750	4.4195	4.2496	3.9770	3.5477	3.1142	1.5289	1.4703	1.3766	1.2763	1.1732
1.5000	4.3401	4.1375	3.7898	3.4042	3.0145	1.4444	1.3939	1.3111	1.2208	1.1268
1.6250	4.1748	3.9872	3.6670	3.3135	2.9547	1.3787	1.3346	1.2605	1.1781	1.0913
1.7500	4.0716	3.8954	3.5952	3.2645	2.9277	1.3265	1.2876	1.2206	1.1446	1.0635
1.8750	4.0166	3.8492	3.5638	3.2494	2.9280	1.2844	1.2496	1.1885	1.1177	1.0413
2.0000	3.9999	3.8393	3.5651	3.2623	2.9515	1.2500	1.2186	1.1623	1.0960	1.0234
2.1250	4.0146	3.8595	3.5936	3.2987	2.9947	1.2214	1.1929	1.1407	1.0780	1.0088
2.2500	4.0557	3.9048	3.6450	3.3552	3.0443	1.1975	1.1713	1.1226	1.0631	0.9966
2.3750	4.1192	3.9717	3.7162	3.3720	3.0003	1.7773	1.1531	1.1073	1.0505	0.9864
2.5000	4.1349	3.9718	3.6715	3.3260	2.9717	1.1600	1.1375	1.0943	1.0398	0.9777

Table 7. Buckling load intensity factor, $k = \sigma t b^2/(\pi^2 D)$, of Mindlin plates having SFSF boundary conditions with a central longitudinal internal line support $\Lambda_1 = \eta - 0.5$ subject to uni- and bi-axial loadings

t/b	Case 9					Case 13				
a/b	0.0010	0.0500	0.1000	0.1500	0.2000	0.0010	0.0500	0.1000	0.1500	0.2000
0.5000	5.6063	5.3709	4.8634	4.2362	3.6022	4.2204	3.9911	3.5703	3.0889	2.6206
0.6250	4.1956	4.0514	3.7596	3.3901	2.9944	2.7954	2.6688	2.4508	2.1963	1.9347
0.7500	3.4310	3.3251	3.1269	2.8771	2.6025	2.0047	1.9237	1.7927	1.6404	1.4798
0.8750	2.9707	2.8840	2.7335	2.5472	2.3402	1.5158	1.4589	1.3719	1.2722	1.1659
1.0000	2.6725	2.5966	2.4732	2.3240	2.1581	1.1898	1.1473	1.0854	1.0156	0.9409
1.1250	2.4683	2.3990	2.2924	2.1667	2.0274	0.9603	0.9272	0.8808	0.8294	0.7745
1.2500	2.3224	2.2574	2.1619	2.0519	1.9308	0.7920	0.7654	0.7293	0.6899	0.6479
1.3750	2.2145	2.1525	2.0648	1.9658	1.8576	0.6646	0.6427	0.6138	0.5826	0.5496
1.5000	2.1325	2.0726	1.9905	1.8996	1.8008	0.5657	0.5474	0.5236	0.4984	0.4717
1.6250	2.0687	2.0105	1.9325	1.8476	1.7560	0.4873	0.4717	0.4518	0.4310	0.4091
1.7500	2.0182	1.9611	1.8864	1.8061	1.7201	0.4241	0.4106	0.3938	0.3762	0.3579
1.8750	1.9774	1.9213	1.8491	1.7724	1.6909	0.3724	0.3607	0.3461	0.3312	0.3156
2.0000	1.9440	1.8887	1.8185	1.7448	1.6668	0.3295	0.3192	0.3066	0.2937	0.2803
2.1250	1.9164	1.8616	1.7931	1.7218	1.6467	0.2936	0.2845	0.2734	0.2621	0.2505
2.2500	1.8932	1.8390	1.7717	1.7024	1.6297	0.2632	0.2551	0.2453	0.2353	0.2251
2.3750	1.8736	1.8198	1.7537	1.6860	1.6153	0.2373	0.2300	0.2212	0.2124	0.2034
2.5000	1.8569	1.8034	1.7383	1.6720	1.6030	0.2150	0.2084	0.2205	0.1927	0.1846

Table 8. Buckling load intensity factor, $k = \sigma t b^2/(\pi^2 D)$, of Mindlin plates having S*FS*F boundary conditions with a central longitudinal internal line support $\Lambda_1 = \eta - 0.5$ subject to uni- and bi-axial loadings

t/b	Case 10					Case 14				
a/b	0.0010	0.0500	0.1000	0.1500	0.2000	0.0010	0.0500	0.1000	0.1500	0.2000
0.5000	5.6060	5.1708	4.5211	3.8296	3.1900	4.2202	3.7996	3.2418	2.6985	2.2230
0.6250	4.1954	3.8916	3.4688	3.0223	2.5954	2.7952	2.5447	2.2282	1.9182	1.6346
0.7500	3.4308	3.1938	2.8754	2.5466	2.2281	2.0046	1.8385	1.6326	1.4331	1.2469
0.8750	2.9706	2.7743	2.5127	2.2490	1.9925	1.5157	1.3985	1.2528	1.1137	0.9828
1.0000	2.6724	2.5036	2.2770	2.0532	1.8356	1.1898	1.1036	0.9948	0.8923	0.7955
1.1250	2.4682	2.3194	2.1165	1.9191	1.7276	0.9603	0.8950	0.8107	0.7321	0.6578
1.2500	2.3223	2.1886	2.0030	1.8241	1.6511	0.7920	0.7412	0.6743	0.6122	0.5535
1.3750	2.2144	2.0925	1.9204	1.7550	1.5955	0.6646	0.6243	0.5702	0.5198	0.4725
1.5000	2.1325	2.0199	1.8588	1.7035	1.5544	0.5657	0.5331	0.4886	0.4471	0.4081
1.6250	2.0687	1.9637	1.8119	1.6646	1.5234	0.4873	0.4605	0.4235	0.3888	0.3561
1.7500	2.0181	1.9194	1.7755	1.6347	1.4997	0.4241	0.4018	0.3707	0.3412	0.3135
1.8750	1.9773	1.8838	1.7468	1.6114	1.4815	0.3724	0.3536	0.3272	0.3019	0.2781
2.0000	1.9440	1.8548	1.7239	1.5931	1.4673	0.3295	0.3135	0.2909	0.2690	0.2484
2.1250	1.9163	1.8308	1.7054	1.5787	1.4562	0.2936	0.2798	0.2603	0.2412	0.2232
2.2500	1.8932	1.8108	1.6902	1.5671	1.4476	0.2632	0.2512	0.2342	0.2175	0.2017
2.3750	1.8736	1.7939	1.6777	1.5579	1.4408	0.2373	0.2268	0.2119	0.1971	0.1831
2.5000	1.8568	1.7795	1.6673	1.5504	1.4355	0.2150	0.2057	0.1926	0.1795	0.1670

Table 9. Buckling load intensity factor, $k = \sigma t b^2/(\pi^2 D)$, of Mindlin plates having SSSS boundary conditions with a central longitudinal internal line support $\Lambda_1 = \eta - 0.5$ subject to uni- and bi-axial loadings

t/b	Case 11					Case 15				
a/b	0.0010	0.0500	0.1000	0.1500	0.2000	0.0010	0.0500	0.1000	0.1500	0.2000
0.5000	15.9997	15.1458	13.0549	10.6131	7.6783	7.9998	7.5729	6.5275	5.3066	4.2053
0.6250	16.8097	16.0671	14.1290	10.4033	7.5982	6.5599	6.2700	5.5360	4.6321	3.7703
0.7500	17.3606	16.1000	13.2193	10.1826	7.6784	5.7777	5.5517	4.9683	4.2279	3.4981
0.8750	16.2866	15.2926	12.9250	10.2740	7.6037	5.3061	5.1148	4.6155	3.9697	3.3194
1.0000	15.9997	15.1458	13.0549	10.2902	7.6136	4.9999	4.8298	4.3822	3.7958	3.1970
1.1250	16.2227	15.4435	13.2193	10.1826	7.6162	4.7901	4.6337	4.2201	3.6736	3.1099
1.2500	16.5374	15.4732	12.9686	10.2133	7.5997	4.6400	4.4930	4.1031	3.5847	3.0459
1.3750	16.1211	15.1838	12.9279	10.2529	7.6289	4.5289	4.3888	4.0160	3.5180	2.9976
1.5000	15.9997	15.1458	13.0549	10.1858	7.6036	4.4444	4.3094	3.9495	3.4669	2.9604
1.6250	16.1025	15.3035	13.0154	10.1962	7.6084	4.3786	4.2476	3.8975	3.4267	2.9311
1.7500	16.2961	15.3006	12.9297	10.2401	7.6422	4.3265	4.1985	3.8561	3.3947	2.9076
1.8750	16.0741	15.1597	12.9490	10.1918	7.6750	4.2844	4.1588	3.8226	3.3687	2.8885
2.0000	16.0059	15.1509	13.0575	10.1929	7.6682	4.2500	4.1264	3.7952	3.3474	2.8728
2.1250	16.0633	15.2519	12.9602	10.2387	7.6785	4.2214	4.0995	3.7724	3.3297	2.8598
2.2500	16.2042	15.2410	12.9335	10.3249	7.7050	4.1975	4.0769	3.7533	3.3147	2.8488
2.3750	16.0635	15.1598	12.9694	10.3392	7.6995	4.1772	4.0578	3.7371	3.3021	2.8394
2.5000	16.0171	15.1598	13.0606	10.3288	7.7035	4.1600	4.0415	3.7232	3.2913	2.8314

Table 10. Buckling load intensity factor, $k = \sigma t b^2/(\pi^2 D)$, of Mindlin plates having S*S*S*S* boundary conditions with a central longitudinal internal line support $\Lambda_1 = \eta - 0.5$ subject to uni- and bi-axial loadings

t/b			Case 12					Case 16		
a/b	0.0010	0.0500	0.1000	0.1500	0.2000	0.0010	0.0500	0.1000	0.1500	0.2000
0.5000	15.9984	14.2610	11.8073	9.4673	7.3796	7.9992	7.1312	5.9069	4.7430	3.7736
0.6250	16.8087	15.2838	12.9883	9.7844	7.1878	6.5595	5.9670	5.0796	4.1899	3.4104
0.7500	17.3599	15.4403	12.3587	9.4727	7.1909	5.7775	5.3372	4.6286	3.8847	3.2073
0.8750	16.2860	14.6742	12.0512	9.4948	7.2878	5.3059	4.9584	4.3574	3.7012	3.0856
1.0000	15.9992	14.5624	12.1751	9.7399	7.2335	4.9998	4.7124	4.1819	3.5829	3.0077
1.1250	16.2223	14.8882	12.5012	9.5795	7.2538	4.7900	4.5434	4.0618	3.5021	2.9550
1.2500	16.5392	14.9901	12.2397	9.5613	7.2766	4.6399	4.4219	3.9756	3.4445	2.9177
1.3750	16.1224	14.7185	12.1904	9.6566	7.2606	4.5288	4.3316	3.9118	3.4019	2.8903
1.5000	16.0007	14.6941	12.3065	9.6301	7.2792	4.4444	4.2625	3.8630	3.3694	2.8695
1.6250	16.1031	14.8604	12.3519	9.6045	7.2790	4.3786	4.2086	3.8248	3.3440	2.8533
1.7500	16.2958	14.8720	12.2583	9.6429	7.2760	4.3265	4.1655	3.7944	3.3238	2.8405
1.8750	16.0738	14.7403	12.2676	9.6595	7.2939	4.2844	4.1306	3.7697	3.3075	2.8302
2.0000	16.0056	14.7387	12.3616	9.6332	7.3022	4.2499	4.1020	3.7493	3.2940	2.8217
2.1250	16.0631	14.8446	12.3309	9.6482	7.2953	4.2214	4.0782	3.7323	3.2828	2.8146
2.2500	16.2258	14.9197	12.2946	9.7008	7.3020	4.1975	4.0582	3.7180	3.2733	2.8087
2.3750	16.3915	14.8335	12.3180	9.7176	7.3236	4.1772	4.0412	3.7058	3.2653	2.8036
2.5000	16.2789	14.8234	12.3939	9.6988	7.3599	4.1599	4.0267	3.6954	3.2583	2.7993

Table 11. Buckling load intensity factor, $k = \sigma t b^2/(\pi^2 D)$, of Mindlin plates having SFSF boundary conditions with central longitudinal and transverse internal line supports $\Lambda_1 = \eta - 0.5$ and $\Lambda_2 = \xi - 0.5$ subject to uni- and bi-axial loadings

t/b			Case 17					Case 21		
a/b	0.0010	0.0500	0.1000	0.1500	0.2000	0.0010	0.0500	0.1000	0.1500	0.2000
0.5000	17.4223	15.4990	11.7710	8.4381	6.0524	15.8789	13.8696	10.3559	7.3931	5.3253
0.6250	11.7421	10.8252	8.8863	6.8799	5.2392	10.2929	9.3351	7.5445	5.8053	4.4255
0.7500	8.6622	8.1432	7.0085	5.7235	4.5675	7.2558	6.7197	5.7013	4.6245	3.6875
0.8750	6.8080	6.4749	5.7445	4.8707	4.0291	5.4189	5.0825	4.4504	3.7475	3.0944
1.0000	5.6063	5.3709	4.8634	4.2362	3.6022	4.2204	3.9911	3.5703	3.0889	2.6206
1.1250	4.7835	4.6044	4.2293	3.7573	3.2639	3.3928	3.2264	2.9302	2.5864	2.2410
1.2500	4.1956	4.0514	3.7596	3.3901	2.9944	2.7954	2.6688	2.4508	2.1962	1.9347
1.3750	3.7611	3.6397	3.4032	3.1038	2.7780	2.3486	2.2487	2.0823	1.8880	1.6851
1.5000	3.4309	3.3251	3.1269	2.8772	2.6025	2.0047	1.9237	1.7927	1.6404	1.4798
1.6250	3.1743	3.0795	2.9087	2.6952	2.4589	1.7337	1.6664	1.5608	1.4388	1.3091
1.7500	2.9707	2.8841	2.7335	2.5472	2.3402	1.5158	1.4589	1.3719	1.2722	1.1659
1.8750	2.8067	2.7261	2.5908	2.4254	2.2413	1.3376	1.2887	1.2159	1.1331	1.0445
2.0000	2.6725	2.5966	2.4732	2.3240	2.1582	1.1898	1.1473	1.0854	1.0156	0.9409
2.1250	2.5614	2.4891	2.3750	2.2389	2.0876	1.0657	1.0284	0.9750	0.9155	0.8517
2.2500	2.4683	2.3990	2.2924	2.1667	2.0274	0.9603	0.9272	0.8808	0.8294	0.7745
2.3750	2.3896	2.3226	2.2221	2.1050	1.9756	0.8700	0.8405	0.7997	0.7549	0.7071
2.5000	2.3224	2.2574	2.1619	2.0519	1.9308	0.7920	0.7654	0.7293	0.6899	0.6479

Table 12. Buckling load intensity factor, $k = \sigma t b^2/(\pi^2 D)$, of Mindlin plates having S*FS*F boundary conditions with central longitudinal and transverse internal line supports $\Lambda_1 = \eta - 0.5$ and $\Lambda_2 = \xi - 0.5$ subject to uni- and bi-axial loadings

t/b			Case 18					Case 22		
a/b	0.0010	0.0500	0.1000	0.1500	0.2000	0.0010	0.0500	0.1000	0.1500	0.2000
0.5000	17.4220	15.3122	11.5400	8.2458	5.9103	15.8783	13.4791	9.7369	6.7941	4.8376
0.6250	11.7419	10.6719	8.6665	6.6689	5.0641	10.2927	9.0989	7.1539	5.3876	4.0497
0.7500	8.6621	8.0146	6.8049	5.5079	4.3721	7.2556	6.5580	5.4260	4.3142	3.3908
0.8750	6.8079	6.3652	5.5574	4.6581	3.8234	5.4188	4.9641	4.2416	3.5031	2.8504
1.0000	5.6062	5.2763	4.6916	4.0307	3.3930	4.2204	3.9009	3.4048	2.8888	2.4136
1.1250	4.7834	4.5221	4.0712	3.5607	3.0556	3.3927	3.1559	2.7954	2.4187	2.0622
1.2500	4.1955	3.9792	3.6138	3.2028	2.7896	2.7953	2.6128	2.3389	2.0535	1.7786
1.3750	3.7611	3.5759	3.2684	2.9258	2.5783	2.3486	2.2036	1.9883	1.7652	1.5481
1.5000	3.4309	3.2685	3.0019	2.7081	2.4087	2.0047	1.8870	1.7131	1.5342	1.3589
1.6250	3.1742	3.0290	2.7925	2.5346	2.2713	1.7337	1.6363	1.4929	1.3463	1.2022
1.7500	2.9707	2.8388	2.6253	2.3945	2.1589	1.5158	1.4340	1.3137	1.1914	1.0710
1.8750	2.8067	2.6853	2.4899	2.2800	2.0662	1.3376	1.2680	1.1658	1.0622	0.9602
2.0000	2.6725	2.5597	2.3788	2.1856	1.9890	1.1898	1.1300	1.0421	0.9532	0.8657
2.1250	2.5614	2.4556	2.2867	2.1068	1.9242	1.0657	1.0137	0.9375	0.8604	0.7846
2.2500	2.4683	2.3684	2.2096	2.0406	1.8695	0.9603	0.9148	0.8481	0.7806	0.7144
2.3750	2.3896	2.2947	2.1444	1.9846	1.8229	0.8700	0.8299	0.7711	0.7116	0.6532
2.5000	2.3224	2.2317	2.0888	1.9367	1.7830	0.7920	0.7564	0.7043	0.6514	0.5996

Table 13. Buckling load intensity factor, $k = \sigma t b^2/(\pi^2 D)$, of Mindlin plates having SSSS boundary conditions with central longitudinal and transverse internal line supports $\Lambda_1 = \eta - 0.5$ and $\Lambda_2 = \xi - 0.5$ subject to uni- and bi-axial loadings

t/b	Case 19					Case 23				
a/b	0.0010	0.0500	0.1000	0.1500	0.2000	0.0010	0.0500	0.1000	0.1500	0.2000
0.5000	24.9988	21.9107	15.9849	11.0183	7.6784	19.9990	17.5287	12.7879	8.8147	6.1427
0.6250	19.8017	17.9960	14.1291	10.4033	7.5982	14.2395	12.9410	10.1602	7.4810	5.4639
0.7500	17.3607	16.1000	13.2193	10.1826	7.7048	11.1108	10.3040	8.4603	6.5169	4.9311
0.8750	16.2866	15.2925	12.9250	10.2740	7.7912	9.2243	8.6613	7.3204	5.8189	4.5208
1.0000	15.9997	15.1458	13.0549	10.6131	7.6804	7.9998	7.5729	6.5275	5.3065	4.2053
1.1250	16.2227	15.4434	13.4976	10.6609	7.6162	7.1604	6.8164	5.9576	4.9236	3.9612
1.2500	16.8097	16.0670	14.1387	10.4077	7.5996	6.5599	6.2701	5.5359	4.6321	3.7703
1.3750	17.6780	16.8853	13.5890	10.2529	7.6299	6.1156	5.8629	5.2162	4.4060	3.6192
1.5000	17.3747	16.1117	13.2262	10.1858	7.7045	5.7777	5.5517	4.9683	4.2279	3.4981
1.6250	16.7109	15.6036	13.0154	10.1962	7.7399	5.5147	5.3084	4.7726	4.0854	3.3999
1.7500	16.2961	15.3005	12.9297	10.2755	7.6991	5.3061	5.1148	4.6155	3.9697	3.3194
1.8750	16.0741	15.1597	12.9490	10.4158	7.6750	5.1377	4.9582	4.4876	3.8747	3.2528
2.0000	16.0059	15.1509	13.0575	10.5432	7.6683	4.9999	4.8298	4.3821	3.7958	3.1970
2.1250	16.0634	15.2518	13.2433	10.4527	7.6785	4.8858	4.7231	4.2942	3.7297	3.1499
2.2500	16.2261	15.4458	13.4867	10.3797	7.7049	4.7901	4.6337	4.2201	3.6736	3.1099
2.3750	16.4786	15.7199	13.5141	10.3391	7.7213	4.7091	4.5579	4.1571	3.6258	3.0755
2.5000	16.8081	15.9499	13.3527	10.3288	7.7362	4.6399	4.4930	4.1031	3.5847	3.0459

Table 14. Buckling load intensity factor, $k = \sigma t b^2/(\pi^2 D)$, of Mindlin plates having S*S*S*S* boundary conditions with central longitudinal and transverse internal line supports $\Lambda_1 = \eta - 0.5$ and $\Lambda_2 = \xi - 0.5$ subject to uni- and bi-axial loadings

t/b	Case 20					Case 24				
a/b	0.0010	0.0500	0.1000	0.1500	0.2000	0.0010	0.0500	0.1000	0.1500	0.2000
0.5000	24.9974	21.1544	15.2318	10.5243	7.3797	19.9979	16.9182	12.1772	8.4149	5.9035
0.6250	19.8008	17.2891	13.3018	9.7844	7.1878	14.2388	12.4297	9.5602	7.0337	5.1721
0.7500	17.3600	15.4403	12.3587	9.4728	7.1909	11.1103	9.8806	7.9079	6.0645	4.6144
0.8750	16.2861	14.6741	12.0513	9.4949	7.3405	9.2240	8.3112	6.8276	5.3867	4.2006
1.0000	15.9991	14.5624	12.1751	9.7623	7.4015	7.9996	7.2826	6.0947	4.9067	3.8956
1.1250	16.2223	14.8882	12.6032	10.0528	7.3302	7.1602	6.5744	5.5799	4.5606	3.6698
1.2500	16.8093	15.5297	13.1467	9.9062	7.2766	6.5597	6.0667	5.2070	4.3057	3.5006
1.3750	17.6775	16.2614	12.9181	9.7306	7.2606	6.1155	5.6908	4.9293	4.1141	3.3722
1.5000	17.3744	15.6533	12.5679	9.6302	7.2792	5.7776	5.4048	4.7175	3.9672	3.2732
1.6250	16.7106	15.1635	12.3519	9.6045	7.3138	5.5146	5.1820	4.5525	3.8524	3.1958
1.7500	16.2958	14.8720	12.2583	9.6428	7.3295	5.3060	5.0052	4.4215	3.7613	3.1342
1.8750	16.0739	14.7404	12.2676	9.7258	7.3181	5.1376	4.8624	4.3159	3.6879	3.0847
2.0000	16.0056	14.7387	12.3617	9.8049	7.3022	4.9999	4.7455	4.2296	3.6278	3.0443
2.1250	16.0631	14.8446	12.5180	9.8061	7.2953	4.8857	4.6486	4.1579	3.5781	3.0110
2.2500	16.2257	15.0403	12.6805	9.7589	7.3020	4.7900	4.5672	4.0979	3.5366	2.9832
2.3750	16.4783	15.3063	12.6936	9.7176	7.3236	4.7091	4.4983	4.0471	3.5014	2.9598
2.5000	16.8077	15.4550	12.5936	9.6988	7.3600	4.6399	4.4394	4.0036	3.4715	2.9398

Table 15. Buckling load intensity factor, $k = \sigma t b^2/(\pi^2 D)$, of Mindlin plates having SFSF boundary conditions with diagonal internal line supports $\Lambda_1 = \eta - \xi$ and $\Lambda_2 = \eta + \xi - 1$ subject to uni- and bi-axial loadings

t/b	Case 25					Case 29				
a/b	0.0010	0.0500	0.1000	0.1500	0.2000	0.0010	0.0500	0.1000	0.1500	0.2000
0.5000	25.3726	20.2691	13.3679	8.9572	6.3018	13.2686	9.9233	6.6860	4.7639	3.5636
0.6250	17.5959	15.2210	11.1975	8.0254	5.8740	8.7509	7.2151	5.2795	3.9204	3.0060
0.7500	13.1935	11.9255	9.4797	7.2216	5.5031	6.2570	5.4604	4.2661	3.3003	2.5993
0.8750	10.5258	9.7670	8.1927	6.5616	5.1888	4.7004	4.2525	3.5008	2.8168	2.2785
1.0000	8.8585	8.3550	7.2722	6.0540	4.9393	3.6717	3.4003	2.9143	2.4297	2.0180
1.1250	7.8101	7.4425	6.6429	5.6903	4.7583	2.9668	2.7912	2.4663	2.1196	1.8045
1.2500	7.1665	6.8738	6.2393	5.4533	4.6433	2.4738	2.3530	2.1270	1.8737	1.6301
1.3750	6.8003	6.5491	6.0095	5.3234	4.5878	2.1237	2.0357	1.8713	1.6807	1.4890
1.5000	6.6315	6.4023	5.9134	5.2805	4.5815	1.8712	1.8039	1.6788	1.5305	1.3758
1.6250	6.6071	6.3872	5.9193	5.3051	4.6115	1.6864	1.6326	1.5333	1.4137	1.2855
1.7500	6.6887	6.4689	5.9996	5.3760	4.6622	1.5490	1.5045	1.4227	1.3229	1.2152
1.8750	6.8447	6.6166	6.1261	5.4688	4.7157	1.4454	1.4074	1.3378	1.2520	1.1566
2.0000	7.0425	6.7968	6.2653	5.5545	4.7568	1.3660	1.3330	1.2721	1.1964	1.1110
2.1250	7.2394	6.9649	6.3753	5.6079	4.7545	1.3045	1.2751	1.2207	1.1524	1.0747
2.2500	7.3775	7.0643	6.4247	5.6245	4.7573	1.2561	1.2297	1.1802	1.1175	1.0454
2.3750	7.4196	7.0871	6.4231	5.6210	4.7697	1.2176	1.1935	1.1478	1.0894	1.0218
2.5000	7.3989	7.0627	6.4036	5.6156	4.7913	1.1867	1.1644	1.1218	1.0668	1.0026

Table 16. Buckling load intensity factor, $k = \sigma t b^2/(\pi^2 D)$, of Mindlin plates having S*FS*F boundary conditions with diagonal internal line supports $\Lambda_1 = \eta - \xi$ and $\Lambda_2 = \eta + \xi - 1$ subject to uni- and bi-axial loadings

t/b			Case 26					Case 30		
a/b	0.0010	0.0500	0.1000	0.1500	0.2000	0.0010	0.0500	0.1000	0.1500	0.2000
0.5000	25.3899	20.1787	13.1345	8.6848	6.0629	13.3260	9.8051	6.4197	4.4505	3.2581
0.6250	17.6081	15.1748	11.0740	7.8589	5.7105	8.7861	7.1708	5.1596	3.7546	2.8288
0.7500	13.2005	11.8894	9.3939	7.1050	5.3845	6.2745	5.4400	4.2061	3.2082	2.4917
0.8750	10.5290	9.7348	8.1223	6.4697	5.0961	4.7112	4.2408	3.4667	2.7616	2.2107
1.0000	8.8595	8.3257	7.2103	5.9762	4.8626	3.6782	3.3921	2.8918	2.3934	1.9728
1.1250	7.8102	7.4162	6.5874	5.6219	4.6925	2.9707	2.7847	2.4496	2.0935	1.7724
1.2500	7.1667	6.8503	6.1892	5.3925	4.5860	2.4762	2.3477	2.1137	1.8537	1.6061
1.3750	6.8010	6.5283	5.9645	5.2691	4.5378	2.1251	2.0313	1.8604	1.6649	1.4703
1.5000	6.6331	6.3840	5.8735	5.2330	4.5392	1.8721	1.8001	1.6697	1.5175	1.3608
1.6250	6.6098	6.3714	5.8849	5.2651	4.5781	1.6869	1.6294	1.5257	1.4029	1.2732
1.7500	6.6926	6.4557	5.9714	5.3454	4.6399	1.5494	1.5018	1.4162	1.3138	1.2034
1.8750	6.8496	6.6065	6.1060	5.4505	4.7066	1.4456	1.4052	1.3323	1.2443	1.1479
2.0000	7.0485	6.7908	6.2556	5.5502	4.7590	1.3662	1.3311	1.2674	1.1898	1.1037
2.1250	7.2468	6.9643	6.3763	5.6122	4.7810	1.3046	1.2735	1.2167	1.1467	1.0683
2.2500	7.3796	7.0374	6.4026	5.6262	4.7876	1.2562	1.2282	1.1767	1.1126	1.0399
2.3750	7.4198	7.0809	6.4250	5.6146	4.7819	1.2177	1.1923	1.1448	1.0852	1.0170
2.5000	7.4157	7.0716	6.4018	5.6015	4.7766	1.1867	1.1633	1.1192	1.0631	0.9985

Table 17. Buckling load intensity factor, $k = \sigma t b^2/(\pi^2 D)$, of Mindlin plates having SSSS boundary conditions with diagonal internal line supports $\Lambda_1 = \eta - \xi$ and $\Lambda_2 = \eta + \xi - 1$ subject to uni- and bi-axial loadings

t/b			Case 27					Case 31		
a/b	0.0010	0.0500	0.1000	0.1500	0.2000	0.0010	0.0500	0.1000	0.1500	0.2000
0.5000	38.4408	30.9807	19.6860	12.2205	7.8591	28.3204	22.8024	14.7102	9.4392	6.3567
0.6250	27.6092	23.8750	16.9557	11.3092	7.5581	19.4043	16.8193	12.1210	8.3570	5.8636
0.7500	22.2887	19.9776	15.1377	10.5886	7.2921	14.4462	13.0425	10.1301	7.4129	5.4047
0.8750	19.5802	17.8386	13.9565	10.0301	7.0555	11.6378	10.7443	8.7378	6.6696	5.0128
1.0000	18.1373	16.6074	13.1454	9.5860	6.8465	9.9997	9.3415	7.8004	6.1182	4.6994
1.1250	17.2007	15.7527	12.5150	9.2187	6.6661	9.0156	8.4714	7.1746	5.7193	4.4565
1.2500	16.3912	15.0156	11.9785	8.9070	6.5095	8.4058	7.9189	6.7531	5.4316	4.2700
1.3750	15.6396	14.3506	11.5148	8.6399	6.3726	8.0125	7.5556	6.4621	5.2207	4.1253
1.5000	14.9873	13.7788	11.1198	8.4099	6.2517	7.7438	7.3033	6.2516	5.0602	4.0098
1.6250	14.4494	13.3036	10.7849	8.2097	6.1414	7.5437	7.1131	6.0881	4.9310	3.9134
1.7500	14.0049	12.9058	10.4965	8.0292	6.0345	7.3780	6.9544	5.9495	4.8194	3.8287
1.8750	13.5918	12.5337	10.2162	7.8496	5.9382	7.2268	6.8093	5.8224	4.7171	3.7509
2.0000	13.1575	12.1530	9.9507	7.6909	5.8525	7.0806	6.6693	5.7006	4.6199	3.6776
2.1250	12.8040	11.8389	9.7258	7.5537	5.7777	6.9371	6.5324	5.5825	4.5267	3.6078
2.2500	12.5339	11.5928	9.5419	7.4378	5.7137	6.7978	6.3999	5.4690	4.4378	3.5417
2.3750	12.2969	11.3816	9.3873	7.3386	5.6509	6.6648	6.2738	5.3615	4.3538	3.4794
2.5000	12.0225	11.1389	9.2126	7.2293	5.5883	6.5392	6.1549	5.2606	4.2752	3.4210

Table 18. Buckling load intensity factor, $k = \sigma t b^2/(\pi^2 D)$, of Mindlin plates having S*S*S*S* boundary conditions with diagonal internal line supports $\Lambda_1 = \eta - \xi$ and $\Lambda_2 = \eta + \xi - 1$ subject to uni- and bi-axial loadings

t/b			Case 28					Case 32		
a/b	0.0010	0.0500	0.1000	0.1500	0.2000	0.0010	0.0500	0.1000	0.1500	0.2000
0.5000	38.4509	30.6512	19.3564	12.0165	7.7698	28.4725	22.4069	14.3018	9.1494	6.1678
0.6250	27.6431	23.5761	16.6176	11.0830	7.4430	19.4839	16.5698	11.8192	8.1220	5.7002
0.7500	22.3692	19.7056	14.7990	10.3481	7.1568	14.4720	12.8540	9.8801	7.2088	5.2587
0.8750	19.7351	17.5882	13.6239	9.7823	6.9032	11.6452	10.5934	8.5215	6.4846	4.8768
1.0000	18.3964	16.3734	12.8235	9.3358	6.6844	10.0030	9.2181	7.6112	5.9484	4.5701
1.1250	17.5586	15.5316	12.2051	8.9683	6.4962	9.0209	8.3687	7.0082	5.5631	4.3331
1.2500	16.7070	14.8058	11.6791	8.6568	6.3333	8.4162	7.8318	6.6060	5.2875	4.1519
1.3750	15.9089	14.1525	11.2246	8.3901	6.1912	8.0302	7.4804	6.3307	5.0872	4.0121
1.5000	15.1930	13.5949	10.8391	8.1612	6.0664	7.7697	7.2369	6.1325	4.9354	3.9007
1.6250	14.5970	13.1394	10.5165	7.9638	5.9487	7.5778	7.0530	5.9780	4.8126	3.8074
1.7500	14.1599	12.7712	10.2248	7.7695	5.8392	7.4184	6.8986	5.8452	4.7053	3.7247
1.8750	13.6624	12.3588	9.9329	7.5930	5.7410	7.2693	6.7564	5.7215	4.6055	3.6481
2.0000	13.2330	11.9932	9.6803	7.4385	5.6542	7.1200	6.6183	5.6017	4.5097	3.5755
2.1250	12.8843	11.6939	9.4693	7.3066	5.5792	6.9694	6.4836	5.4856	4.4177	3.5063
2.2500	12.6188	11.4620	9.3000	7.1972	5.5157	6.8230	6.3543	5.3750	4.3305	3.4408
2.3750	12.4335	11.2944	9.1706	7.1095	5.4636	6.6865	6.2329	5.2716	4.2489	3.3795
2.5000	12.3180	11.1855	9.0782	7.0425	5.4225	6.5635	6.1209	5.1748	4.1734	3.3225

6. CONCLUDING REMARKS

The buckling analysis of rectangular Mindlin plates can be readily performed using the pb-2 Rayleigh–Ritz method. The method can handle any number of arbitrarily oriented/shaped internal supports. This paper tabulates some new buckling load intensity factors for rectangular Mindlin plates with various loading conditions, edge support conditions and orientations of internal line supports.

It is important to note the large decreases in buckling load intensity factors with respect to increasing t/b ratios and some aspect ratios, especially for small a/b ratios. The results obtained show that classical thin plate theory overpredicts the buckling capacities of such plates and can even lead to unsafe designs.

REFERENCES

Column Research Committee of Japan (1971). *Handbook of Structural Stability*. Corona, Tokyo.

Felippa, C. A. (1975). Solution of linear equations with skyline-stored symmetric matrix. *Comput. Struct.* **5**, 13–29.

Hinton, E. (1988). *Numerical Methods and Software for Dynamic Analysis of Plates and Shells*. Pineridge Press, Swansea, U.K.

Huang, H.-C. (1989). *Static and Dynamnic Analysis of Plates and Shells*. Springer, Berlin.

Levinson, M. (1980). An accurate simple theory of the statics and dynamics of elastic plates. *Mech. Res. Commun.* **7**, 343–350.

Libove, C. (1962). Elastic stability. In *Handbook of Engineering Mechanics* (Edited by W. Flugge), Ch. 4. McGraw-Hill, U.S.A.

Liew, K. M. and Wang, C. M. (1992a). pb-2 Rayleigh–Ritz method for general plate analysis. *Engng Struct.* **14** (in press).

Liew, K. M. and Wang, C. M. (1992b). Elastic buckling of rectangular plates with curved internal supports. *J. Struct. Engng ASCE* **118**(6), 1480–1493.

Lim, S. P., Senthilnathan, N. R. and Lee, K. H. (1989). Rayleigh–Ritz vibration analysis of thick plates by a simple higher order theory. *J. Sound Vibr.* **130**, 163–166.

Mindlin, R. D. (1951). Influence of rotary inertia and shear in flexural motion of isotropic, elastic plates. *J. Appl. Mech.* **18**, 1031–1036.

Murthy, M. V. V. (1981). An improved transverse shear deformation theory for laminated anisotropic plate. NASA Technical Paper 1903.

Reddy, J. N. (1984). A simple higher-order theory for laminated composite plates. *J. Appl. Mech. ASME* **51**, 745–752.

Reissner, E. (1945). The effect of transverse shear deformation on the bending of elastic plate. *J. Appl. Mech. ASME* **12**, 69–76.

Roufaeil, O. L. and Dawe, D. J. (1982). Rayleigh–Ritz vibration analysis of rectangular Mindlin plates subjected to membrane stresses. *J. Sound Vibr.* **85**, 263–275.

Senthilnathan, N. R., Lim, S. P., Lee, K. H. and Chow, S. T. (1987). Buckling of shear deformable plates. *AIAA Jl* **25**, 1268–1271.

Srinivas, S. and Rao, A. K. (1969). Buckling of thick rectangular plates. *AIAA Jl* **7**, 1645–1646.

Srinivas, S. and Rao, A. K. (1970). Bending, vibration and buckling of simply supported thick orthotropic rectangular plates and laminates. *Int. J. Solids Structures* **6**, 1463–1481.

Wang, C. M., Liew, K. M. and Alwis, W. A. M. (1992). On buckling of skew plates and corner condition for simply supported edges. *J. Engng Mech. ASCE* **118**(4), 651–662.

Wang, C. M., Xiang, Y. and Kitipornchai, S. (1991). Buckling of restrained columns with shear deformation and axial shortening. *J. Engng Mech. ASCE* **117**, 1973–1989.